MCMV based vaccine vectors expressing full-length viral proteins provide long-term humoral immune protection upon a single-shot vaccination

Luka Cicin-Sain (Luka.Cicin-Sain@helmholtz-hzi.de)
Helmholtz Centre for Infection Research https://orcid.org/0000-0003-3978-778X

Yeonsu Kim
Helmholtz Centre for Infection Research

Xiaoyan Zheng
Helmholtz Centre for Infection Research

Kathrin Eschke
Helmholtz Centre for Infection Research

M. Zeeshan Chaudhry
Helmholtz Centre for Infection Research https://orcid.org/0000-0002-1372-4257

Federico Bertoglio
Institut für Biochemie, Biotechnologie und Bioinformatik, Technischen Universität Braunschweig

Adriana Tomic
University of Oxford

Markus Hoffmann
Georg-August-University Göttingen https://orcid.org/0000-0003-4603-7696

Yotam Bar-On
Rappaport Faculty of Medicine, Technion - Israel Institute of Technology

Julia Boehme
Helmholtz-Centre for Infection Research

Dunja Bruder
Otto-von-Guericke University

Thomas Ebensen
Helmholtz Centre for Infection Research

Linda Brunotte
University Hospital Muenster

Stephan Ludwig
Institute of Virology (IVM), Westfaelische Wilhelms Universitaet, Muenster, Nordrhein-Westfalen, 48149
https://orcid.org/0000-0003-4490-3052

Martin Messerle
Hannover Medical School (MHH)

Carlos Guzmán
Helmholtz Centre for Infection Research
Ofer Mandelboim
The Hebrew University Hadassah Medical School
Michael Hust
Technische Universität Braunschweig https://orcid.org/0000-0003-3418-6045
Stefan Pöhlmann
German Primate Center - Leibniz Institute for Primate Research https://orcid.org/0000-0001-6086-9136
Stipan Jonjic
Univesity of Rijeka, Faculty of Medicine https://orcid.org/0000-0001-5003-3108

Article

Keywords: Cytomegalovirus, Antigen-specific CD8+ T Cells, Neutralizing Antibody Responses, Memory T Cells

Posted Date: June 3rd, 2021

DOI: https://doi.org/10.21203/rs.3.rs-566785/v1

Version of Record: A version of this preprint was published at Cellular & Molecular Immunology on January 7th, 2022. See the published version at https://doi.org/10.1038/s41423-021-00814-5.

MCMV based vaccine vectors expressing full-length viral proteins provide long-term humoral immune protection upon a single-shot vaccination

Yeonsu Kim[1]*, Xiaoyan Zheng[1]*, Kathrin Eschke[1]*, M. Zeeshan Chaudhry[1]*, Federico Bertoglio[2], Adriana Tomic[3], Markus Hoffmann[4a,4b], Yotam Bar-On[5], Julia Boehme[6], Dunja Bruder[6], Thomas Ebensen[7], Linda Brunotte[8], Stephan Ludwig[8], Martin Messerle[9], Carlos Guzman[7], Ofer Mandelboim[10], Michael Hust[2], Stefan Pöhlmann[4a,4b], Stipan Jonjic[3], Cicin-Sain-Luka[1,11,12†]

1. Department for Immunology of Clinically Relevant Infections, Helmholtz Centre for Infection Research (HZI), Braunschweig, Germany
2. Department of Biotechnology, Institut für Biochemie, Biotechnologie und Bioinformatik, Technischen Universität Braunschweig, Braunschweig, Germany
3. Oxford Vaccine Group, University of Oxford, UK.
4. a: Infection Biology Unit, German Primate Center, Göttingen, Germany; b: Faculty of Biology and Psychology, Georg-August-University Göttingen, Göttingen, Germany
5. Department of Immunology, Rappaport Faculty of Medicine, Technion - Israel Institute of Technology, Haifa, Israel.
6. Infection Immunology, Institute for Medical Microbiology and Hospital Hygiene, Health Campus Immunology, Infectiology and Inflammation, Otto-von-Guericke-University Magdeburg, Magdeburg, Germany; Immune Regulation, Helmholtz Centre for Infection Research, Braunschweig, Germany
7. Department of Vaccinology and Applied Microbiology, Helmholtz Centre for Infection Research, Braunschweig, Germany
8. Institute of Virology, Medical University Münster, Germany
9. Institute of Virology, Hannover Medical School (MHH), Hannover, Germany
10. The Lautenberg Center for General and Tumor Immunology, the Faculty of Medicine, IMRIC, The Hebrew University Medical School, Jerusalem

11. German Centre for Infection Research (DZIF), Hannover-Braunschweig Site, Germany
12. Centre for Individualized Infection medicine (CiiM), a joint venture of HZI and MHH, Hannover, Germany

* these authors have contributed equally

† Corresponding author: luka.cicin-sain@helmholtz-hzi.de

Author Contributions

Study conception and design: Y.K., X.Z, K.E., L.C.-S. Methodology: Y.K., K.E., M.Z.C., F.B., M.Ho., X.Z.; Analysis and Interpretation of Results: Y.K. M.Ho. and X.Z. Investigation: Y.K., X.Z., M.Z.C., K.E., F.B., M.Ho., A.T., Y.B.-O., J.B., T.E.; Original Draft Preparation: Y.K. and X.Z.; Draft Review & Editing: Y.K. and L.C.-S.; Final edition: Y.K., M.Z.C., and L.C.-S.; Supervision: D.B., C.G.,O.M., M.Hu., S.P., S.J. and L.C.-S.; Resources, L.B., S.L., and M.M. All authors reviewed the results and approved the final version of the manuscript.

Abstract

Global pandemics by influenza or coronaviruses cause severe disruptions to the public health and lead to severe morbidity and mortality. Vaccines against these pathogens remain a medical need. CMV (cytomegalovirus) is a β-herpesvirus that induces uniquely robust immune responses, where outstandingly large populations of antigen-specific $CD8^+$ T cells are maintained for a lifetime. Hence, CMV has been proposed and investigated as a novel vaccine vector expressing antigenic peptides or proteins to elicit protective cellular immune responses against numerous pathogens. We generated two recombinant murine CMV (MCMV) vaccine vectors expressing the hemagglutinin (HA) of influenza A virus ($MCMV^{HA}$) or the spike protein of the severe acute respiratory syndrome coronavirus 2 ($MCMV^{S}$). A single shot of MCMVs expressing either viral protein induced potent neutralizing antibody responses, which strengthened over time.

Importantly, MCMV^{HA} vaccinated mice were protected from illness following challenge with the influenza virus, and we excluded that this protection was due to effects of memory T cells. Conclusively, we show here that MCMV vectors do not only induce long-term cellular immunity, but also humoral responses that provide long-term immune protection against clinically relevant respiratory pathogens.

Introduction

Severe acute respiratory syndrome coronavirus 2 (SARS-CoV-2) and influenza A virus (IAV) are well-known viruses with a zoonotic origin, causing global pandemics with severe consequences on human health and economies. SARS-CoV-2, which causes coronavirus disease 2019 (COVID-19) pandemics, was first identified in late 2019 in Wuhan, China and has caused a severe global pandemic, which has claimed millions of lives and resulted in severe economic disruption worldwide. Influenza pandemics have also resulted in global disruptions, such as the H1N1 Spanish flu in 1918, H3N2 Hong Kong flu in 1968 and H1N1dpm09 Swine flu in 2009, resulting in rapid global spread of this respiratory disease. In addition to these influenza pandemics, seasonal influenza epidemics regularly cause elevated morbidity and mortality in the colder seasons. Both IAV and SARS CoV-2 may cause mild to severe respiratory illnesses, and pose a particular threat to risk groups, such as the elderly or people with pre-existing medical conditions. Both of these respiratory viruses depend on a viral surface protein for attachment and entry into host cells. In case of IAV, the viral hemagglutinin (HA) is the major surface glycoprotein required for cell entry (1, 2). Likewise, SARS-CoV-2 uses the spike protein (S) to bind its cellular receptor ACE2 and to drive membrane fusion during virus entry (3-6). Therefore, SARS-CoV-2 S and IAV HA are the main antigenic targets in vaccine formulations against these viruses.

Numerous efforts are underway to counter COVID-19. There are more than 200 vaccine projects targeting SARS-CoV-2 (7) using formulations that include viral proteins, viral vector vaccines, and mRNA vaccines. Some of these vaccines have already been approved for use in humans or are in advanced clinical trials with promising results. However, all of the candidates raise safety concerns due to side effects like fever, fatigue and headache (8) and most vaccines (or vaccine candidates) require a prime/boost vaccination protocol at multiple week intervals, raising issues of delivery logistics and compliance. Although mRNA vaccines show great promise in the context of the COVID-19 pandemic (9), the experience with their use in clinical settings remains limited (10). Vaccines against influenza target the predicted prevailing strains in each upcoming flu season, and are especially recommended for people at high risk, such as children, elderly and the immunocompromised (11). While influenza vaccines are available, their efficiency is about 19-60%, depending on the flu season (12, 13).

Viral vectors do not need adjuvants, because they contain molecular patterns recognized by the innate immune receptors and naturally induce both the cellular and the humoral branch of the adaptive immune response (14, 15). Therefore, they are developed by numerous research labs, using a variety of viral vectors, including poxviruses, adenoviruses or herpesviruses, just to name a few (16-25). Among them, cytomegalovirus (CMV) is a highly promising platform for vaccine design, with several advantages and unique features. CMV infection is usually asymptomatic, but the virus persists for life, inducing a strong and durable inflationary $CD8^+$ T-cell response (26-32). The optimal design of CMV-based vaccines is an area of intensive study. Numerous studies on CMV vaccines benefit from powerful $CD8^+$ T-cell responses induced by CMV infection. Various experimental CMV vectors expressing single epitopes against diverse pathogens provided immune protection that was based on robust epitope-specific $CD8^+$ T-cell response (18, 20, 21, 28, 33-37). In alignment with this strategy, boosting or maintaining strong $CD8^+$ T-cell populations, but diminishing viral pathogenesis, was another focus of the CMV vaccine vector design (38-42).

Interestingly, an MCMV vector encoding a $CD8^+$ T-cell epitope derived from the IAV HA gene (43) induced protective $CD8^+$ T-cell responses against IAV, but only when administered intranasally and eliciting responses from mucosa resident $CD8^+$ T cells (37), which was similar to effects observed upon immunization with an MCMV vector targeting an epitope of the respiratory syncytial virus (44).

In this study, we constructed recombinant MCMVs expressing either the full-length IAV HA protein ($MCMV^{HA}$), or SARS-CoV-2 S protein ($MCMV^{S}$). We used these vectors to immunize mice and analyzed their immunoprotective effects. We also compared the $MCMV^{HA}$ immune protection to those induced by a vector expressing the optimally positioned immunodominant epitope from the same virus. We show that immunization with MCMVs expressing a full-length-protein efficiently induced neutralizing antibodies and protected the animals against viral challenge despite poor $CD8^+$ T cell-responses. Experiments in B-cell deficient JHT mice demonstrated that the immune protection conferred by a single-dose administration of the MCMV vector was not only robust and lasting, but also antibody-dependent. This advances the design of MCMV-based vaccines.

Materials and Methods

Ethics statement

BALB/cJRj and C57BL/6JRj mice were purchased from commercial vendors (Janvier, Le Genest Saint Isle, France). B6.129P2-*Igh*-J^{tm1Cgn}/J (JHT) mice were bred in the animal facility of Helmholtz Center for Infection Research, Braunschweig. Animals were housed under SPF conditions at HZI or Hebrew University in Jerusalem and handled according to the good animal practice as defined by Federation of Laboratory Animal Science Associations (FELASA). Animal experiments were approved by the Lower Saxony State Office of Consumer Protection and Food Safety and Hebrew University Medical School Ethic committee.

Cell culture and viruses

Vero E6 (CRL-1586), Vero76 (ATCC CRL-1586), 293T (DSMZ ACC-635), MDCK (CCL-34) and M2-10B4 cells (ATCC CRL-1972) were cultured in DMEM (Gibco, NY, USA) supplemented with 10% fetal bovine serum (FBS), 2 mM L-glutamine, 100 IU/mL penicillin and 100 µg/mL streptomycin. C57BL/6 primary mouse embryo fibroblast (MEF) cells were prepared in-house from C57BL/6JRj mice. The PR8M variant of Influenza A/PR/8/34 was obtained from the strain collection at the Institute of Molecular Virology, Muenster, Germany. SARS-CoV-2 South Tyrol strain (FI strain, hCoV-19/Germany/Muenster_FI1103201/2020, GISAID database ID: EPI_ISL_463008) was isolated by Stephan Ludwig lab. MCMV^{WT} refers to the BAC-derived molecular clone (pSM3fr-MCK-2fl clone 3.3) (Jordan et al., 2011).

Virus mutagenesis

MCMV virus mutants are based on the BAC molecular clone pSM3fr-MCK-2fl clone 3.3, where recombinant variants were generated by *en passant* mutagenesis, as described previously (45, 46). The construction of MCMV^{IVL} has been described previously (37).

MCMV variants expressing the hemagglutinin protein were constructed using either the wild-type MCMV genome or the Δm152-RAE1γ MCMV genome (Slavuljica et al., 2010) to generate $MCMV^{HA}$ and $Rae\text{-}1\gamma MCMV^{HA}$. $MCMV^{HA}$ was generated by replacing m157 ORF with an expression cassette containing the human CMV major immediate-early enhancer and promotor (hMIEP), the hemagglutinin ORF (Fig. S4A). The hemagglutinin ORF was amplified from pUC18 vector containing the hemagglutinin ORF of the PR8 strain (UniProt P03452) that was kindly provided by Peter Stäheli. Recombinant MCMV expressing SARS-CoV-2 spike was generated by inserting the spike ORF in place of the ie2 gene by replacing the start and stop codon of the spike ORF with the start and stop codon of the ie2 ORF. The spike ORF was amplified from pCG1-SARS-2-S plasmid (4, 6) that harbors the spike ORF from the Wuhan-1 strain (GenBank: MN_908947).

Virus stock generation and plaque assay

BAC-derived mutant MCMVs were propagated on M2-10B4 cells and purified by sucrose density gradient as described previously (46). Influenza virus was generated and infectious virus quantified as described previously (37). SARS-CoV-2 virus stocks were generated essentially as described (47). Briefly, infected Vero E6 cells and supernatants were harvested, centrifuged to remove the cell debris and concentrated by Vivaspin® 20 concentrators (Sartorius, Goettingen, Germany) according to manufacturer's instructions. Infectious titer was determined by serially diluting the virus stocks, followed by infection of Vero E6 monolayers in 24-well plates for an hour at 37 ˚C. Thereupon, the inoculum was removed and the cells overlaid with 1.5 % methylcellulose. Cells were incubated at 37˚C for 4 days, fixed with 6% PFA for an hour, stained with crystal violet, and plaque numbers were counted under an inverted microscope.

158 **Virus *in vivo* infection**

159 Female BALB/c mice aged 7-8 weeks were intraperitoneally (i.p.) immunized with $2x10^5$ PFU of
160 recombinant MCMVs expressing antigens or with parental control virus diluted in PBS (200 µl per
161 animal). Blood was acquired at indicated time points.

162 For B-cell depleted animal challenge experiments, 6-8 weeks old BALB/c and JHT female mice
163 were i.p. immunized with $2x10^5$ PFU $MCMV^{HA}$ or $MCMV^{IVL}$ diluted in PBS. For influenza infection,
164 mice were first anesthetized with ketamine (10 mg/ml) and xylazine (1 mg/ml) in 0.9% NaCl (100
165 µl/10 g body weight), then challenged intranasally with 1100 FFU of PR8M influenza virus as
166 described previously (37).

167 Rae-1γ$MCMV^{HA}$ immunizations were performed by infecting C57BL/6 mice via f.p. route with
168 $2x10^5$ PFU of indicated recombinant MCMVs. 21 days post immunization mice were challenged
169 via i.n. route with either high (100 hemagglutinin units, HU) or low dose (40 HU) of PR8M influenza
170 virus.

171 **Detection of anti-spike antibodies in mouse sera**

172 ELISA (Enzyme-Linked ImmunoSorbent Assay) was used to detect SARS-CoV-2 Spike-specific
173 IgGs presence in mouse sera. Antigens were produced in insect cells using a baculovirus-free
174 system according to previous publications (48) and immobilized (30ng/well) in carbonate buffer
175 (50 mM $NaHCO_3/Na_2CO_3$, pH 9.6) at 4°C overnight. ELISA plates were blocked with 2% (w/v)
176 milk powder and 0.05% Tween-20 in PBS (2% MBPST) and washed with 0.05% Tween20 in H_2O.
177 To determine IgG titers, mouse sera were diluted 1:100 in 2% MBPST and further titrated in an
178 ELISA assay using S1-S2-His and RBD-SD1-HIS as antigens or BSA as control for unspecific
179 binding. In addition, all sera were also tested at the highest concentration for unspecific cross-
180 reactivity on Expi293F cell lysate and lysozyme (both 30 ng/well). After 1h incubation at 37°C and
181 washing as reported above, mouse IgGs were detected using goat anti-mouse serum conjugated

with horseradish peroxidase (HRP) (Sigma-Aldrich, Munich, Germany). Bound antibodies were visualized with tetramethylbenzidine (TMB) substrate. After stopping the reaction by addition of 5% H_2SO_4, absorbance at 450 nm with a subtracted 620 nm reference was measured in an ELISA plate reader (Epoch, BioTek, Winooski, VT, USA). Titration assays were performed using 384 well microtiter plates (Greiner, Kremsmuenster, Austria) using Precision XS microplate sample processor (BioTek, Winooski, VT, USA), EL406 washer dispenser (BioTek, Winooski, VT, USA) and BioStack Microplate stacker (BioTek, Winooski, VT, USA). EC_{50} were calculated with GraphPad Prism Version 6.1, fitting to a four-parameter logistic curve.

Antibody avidity assay

Antibody avidity determination was performed essentially as reported previously (49). ELISA 96-well plates (Costar, Corning, NY, USA) were used to immobilize SARS-CoV-2 S1-S2-HIS ectodomain at 100 ng/well in carbonate buffer (50 mM $NaHCO_3/Na_2CO_3$, pH 9.6) at 4°C overnight. After blocking in 2%MPBST, mouse sera were pooled to a final dilution of 1:300 in 2% MPBST and incubated 1h at 37°C on immobilized S1-S2-HIS. After washing with PBS with 0,05% Tween 20, v/v (PBST), plates were incubated with indicated dilutions of NaSCN for 15 min at room temperature, 350 rpm, followed by immediate washing with PBST. IgGs were detected using anti-mouse serum conjugated with HRP (A0168, Sigma-Aldrich, Munich, Germany) and absorbance was measured as described above. Values obtained in absence of NaSCN were normalized to represent 100% of IgG binding. Hence, the avidity of Spike-specific antibodies was calculated from the ratio of the absorbance of antibodies bound after treatment with graded concentrations of NaSCN relative to the signal in NaSCN absence. One way ANOVA to compare multiple groups was performed with Dunnett's correction for multiple analyses.

Hemagglutination Inhibition Assay (HAI)

Serum samples were derived from mice at day 28 post $MCMV^{HA}$ or $MCMV^{IVL}$ immunization (dpi), or at day 5 after IAV challenge. Sera were tested for HA-specific antibody titers by standard methods using a 0.7% v/v turkey erythrocyte suspension, as described previously (50). In brief, to remove non-specific inhibitors, sera were treated 1:5 and 1:2, respectively with receptor-destroying enzyme (Seiken, Tokyo, Japan) overnight, before heat-inactivation (56°C, 30 min). Sera samples were added to 96-well v-bottomed microtiter plates at a starting dilution of 1:10. The serum HI titers are expressed as the reciprocal of the highest dilution at which 50% hemagglutination was inhibited. A surrogate correlate of protection was extrapolated from seasonal vaccination in humans, using a titer above ≥40 to indicate sero-protection and a serum titer less than 5 as negative result.

In vitro serum neutralization titer (SNT) assay

Serum was heat-inactivated for 30 min at 56˚C, serially diluted at 1:2 steps and incubated with 100PFU/100µl of SARS-CoV-2 for an hour at RT. For IgM depletion, heat-inactivated sera were incubated with 2-ME for an hour at RT prior to mixing with the virus. $2x10^4$ Vero-E6 cells seeded in 96-well plates were inoculated with serum and virus and incubated at 37°C and 5% CO_2 for 1h. After removing the inoculum, cells were overlaid with 1.5% methylcellulose. Infected cells were incubated at 37°C and 5% CO_2 for 3 days, prior to crystal violet staining and plaque counting.

Pseudovirus neutralization assay

We used vesicular stomatitis virus (VSV) pseudotyped with SARS-CoV-2 S according to a published protocol (51) and described in detail previously (52). In brief, 293T cells were transfected with expression plasmids for SARS-CoV-2 S proteins of either Wuhan/Hu-1/2019 (lineage B, with D614G mutation inserted, codon-optimized), hCoV-19/England/MILK-9E05B3/2020 (lineage B.1.1.7, codon-optimized), or hCoV-19/South Africa/NHLS-UCT-GS-1067/2020 (lineage B.1.351, codon-optimized) or empty expression vector (negative control, used

to generate bald control particles) by the calcium-phosphate method. At 24h posttransfection, the transfection medium was removed and cells were inoculated with a replication-deficient VSV vector lacking the genetic information for the VSV glycoprotein (VSV-G) and instead coding for an enhanced green fluorescent protein and firefly luciferase from independent transcription units, VSV*ΔG-FLuc (kindly provided by Gert Zimmer, Institute of Virology and Immunology, Mittelhäusern, Switzerland) (53). Following 1h of incubation at 37°C and 5% CO_2, the inoculum was removed and cells were washed with PBS, before culture medium containing anti-VSV-G antibody (culture supernatant from I1-hybridoma cells; ATCC CRL-2700) was added and cells were further incubated. The pseudotype particles were harvested at 16-18h post-inoculation. For this, the culture medium was collected, centrifuged (2,000 x g, 10 min, RT) to pellet cellular debris, and the clarified supernatant was transferred into fresh tubes and stored at -80°C until further use. Each batch of pseudotypes was pre-tested for comparable transduction efficiencies by the respective S proteins and absence of transduction by control particles lacking any surface glycoprotein before being used in neutralization experiments.

For neutralization experiments, equal volumes of pseudotype particles and serum dilution or medium (control) were mixed and incubated for 30 min at 37°C before being inoculated onto Vero76 cells grown in 96-well plates (100 µl/well, samples were analyzed in technical triplicates). Transduction efficiency, was analyzed at 16h post-transduction. For this, the medium was aspirated and cells were lysed by incubation with Cell Culture Lysis Reagent (Promega, Madison, WI, USA) for 30 min. Lysates were transferred in white 96-well plates and luciferase activity was measured by adding a commercial substrate (Beetle Juice, PJK, Kleinblittersdorf, Germany) and recording the luminescence signals (given as counts per second) with a Hidex Sense plate luminometer (Hidex, Okegawa, Victoria).

252 **Influenza virus *ex vivo* titration**

253 Mice were sacrificed by CO_2 inhalation. Entire lungs were dissected and mechanically
254 homogenized using a tissue homogenizer. Homogenates were spun down and supernatants were
255 stored at -70°C. Lung virus titers were determined by using the focus-forming assay (FFA), as
256 described before (54) with minor modifications. Supernatants of lung tissue homogenates were
257 serially diluted in DMEM, supplemented with 0.1% BSA and N-acetylated trypsin (NAT; 2.5 µg/ml),
258 and added to the MDCK cell monolayers. After 1h incubation, cells were overlaid with DMEM
259 supplemented with 1% Avicel, 0.1% BSA and NAT (2.5 µg/ml). After 24 h, cells were fixed with
260 4% PFA and incubated with quenching solution (0.5% Triton X-100, 20 mM Glycin in PBS). Cells
261 were then treated with blocking buffer (1% BSA, 0.5% Tween-20 in PBS). Focus forming spots
262 were identified using primary polyclonal goat anti-H1N1 IgG (Virostat, Westbrook, ME, USA),
263 secondary polyclonal rabbit anti-goat IgG conjugated with horseradish peroxidase and
264 TrueBlue™ peroxidase substrate (KPL TrueBlue™, SeraCare Life Science Inc., Milford, MA,
265 USA). Viral titers were calculated as focus forming units (FFU) per ml of lung tissue homogenate.

266 **Quantification of T cell responses**

267 Peripheral blood was harvested and lymphocytes were isolated as described previously (Oduro
268 et al., 2016). PBMCs were stimulated with peptide at 1 µg/ml in 85 µl RPMI 1640 for 1h at 37°C,
269 upon which 15 µl brefeldin A (10 µg/ml) was added and cells incubated for additional 5h at 37°C.
270 Lymphocytes were stained with fluorescent-labeled antibodies against CD3 (17A2, eBiosciences,
271 San Diego, CA, USA), CD4 (GK1.5, BioLegend, San Diego, CA, USA), CD8a (53-6.7, BioLegend,
272 San Diego, CA, USA), CD44 (IM7, BioLegend, San Diego, CA, USA) and CD11a (2D7,
273 Bioscience, San Diego, CA, USA). Subsequently, cell were fixed and permeabilized (IC fixation
274 buffer and permeabilization buffer, eBioscience, San Diego, CA, USA) and intracellular cytokines
275 were labelled with anti-IFNγ (XMG1.2, BioLegend, San Diego, CA, USA) and anti-TNFα (MP6-

XT22, BioLegend, San Diego, CA, USA) antibodies. The labeled cells were analyzed by flow cytometry and antigen specific CD8+ T cell response was measured.

Western blot

Sucrose-cushion purified viruses were diluted with PBS and then used to measure protein amount by BCA assay according to the manufacturer's protocol (Pierce™ Micro BCA™ Protein-Assay, ThermoFisher, Waltham, MA, USA). Samples were treated with 2-mercaptoethanol and sample reducing buffer, and then incubated at 95˚C for 5 min. Proteins were separated by SDS-PAGE, transferred on an Immobilon-P PVDF membrane (MilliporeSigma, Munich, Germany) and blocked with 5% milk in TBS-T. Primary antibodies were allowed to bind overnight at 4˚C, followed by a wash in TBS-T and secondary antibody binding for an hour at RT. Upon another wash, the images were acquired by Chemostar PC ECL & Fluorescence Imager (Intas Science, Goettingen, Germany). Anti-SARS-CoV-2 spike (1A9, GeneTex, Irvine, CA, USA), anti-HA (kindly provided by W. Gerhard from Philadeplhia), anti-MCK-2 (kindly provided from Stipan Jonjic) and IE1 (IE 1.01, CapRi, Rijeka, Croatia) were used for primary antibodies. Anti-rabbit IgG (ab205718), anti-mouse IgG (ab97046) were used for secondary antibodies.

Statistics

Comparisons between two groups were performed using the Mann-Whitney U test (two-tailed). One way ANOVA with Dunnett's correction was performed for multiple group analysis. Two-way ANOVA analysis was used to compare multiple groups at multiple time points. Statistical analysis was calculated by GraphPad Prism 6-9.

Results

Generation of recombinant MCMVs expressing the influenza hemagglutinin or the SARS Cov-2 S protein

We recently showed that $MCMV^{IVL}$, a recombinant MCMV vaccine expressing the $_{533}$IYSTVASSL$_{541}$ epitope (IVL) from the IAV HA protein, protects against influenza challenge when administered intranasally by inducing mucosal resident $CD8^+$ T cells (37). We considered the possibility that a recombinant MCMV expressing the full-length HA may provide a similar or better immune protection. Therefore, we generated a recombinant MCMV expressing the full-length HA using a BAC containing the MCMV genome (pSM3fr-MCK-2fl), where the viral m157 gene, which is dispensable for virus *in vivo* replication (55), was replaced with the whole HA gene (Fig. 1A). Since MCMV vectors expressing ligands for the activating NKG2D receptor show improved immune protection over parental viruses (39), we generated another recombinant MCMV that expressed the Rae-1γ ligand instead of the MCMV gene m152 in addition to the IAV HA gene in the m157 locus and named it Rae-1γ$MCMV^{HA}$ (Fig. S1A).

We also generated a recombinant MCMV expressing the gene for the S protein. We replaced the immediate early 2 (ie2) gene of MCMV with the S gene of SARS-CoV-2, because ie2 is dispensable for viral replication and dissemination (56). Thus, using BAC-based recombination we generated a new recombinant virus called $MCMV^S$ (Fig. 1B). The HA and S proteins were detected by Western blot in the purified virus stocks of $MCMV^{HA}$ or $MCMV^S$, respectively (Fig. 1C and 1D) and grew with similar kinetics as the wild-type virus (not shown).

Immunization with MCMV expressing the full-length S protein induces neutralizing antibody responses.

BALB/c mice were i.p. immunized with $MCMV^S$, $MCMV^{WT}$, or PBS (mock). Blood was collected at 7, 14, 28 and 56 dpi and sera were tested for antigen specific responses against the entire S

protein or the receptor binding domain (RBD) by ELISA. We observed notable serum responses in mice immunized with $MCMV^S$ at all indicated time points, peaking by 28 dpi (Fig. 2A).

We next tested the serum neutralization capacity. We used recombinant vesicular stomatitis virus (VSV) expressing the S gene of SARS CoV-2 isolates hCoV-19/Wuhan/WH01/2019 (B lineage, with introduced D614G mutation) hCoV-19/England/MILK-9E05B3/2020 (B.1.1.7 lineage) or hCoV-19/South Africa/NHLS-UCT-GS-1067/2020 (B.1.351 lineage). Following SARS-CoV-2 S protein-driven cell entry, the pseudoviruses express firefly luciferase, which was used as an indicator of infectivity and to analyze the neutralization capacity of the mouse sera. We tested five mouse sera collected 56 days post $MCMV^S$ inoculation and observed an average pseudovirus neutralization titer ($pVNT_{50}$) of 1:900 for pseudotypes bearing either SARS-CoV-2 S WH01+D614G or B.1.1.7, and a slightly reduced, but still robust $pVNT_{50}$ of 1:450 for particles harboring SARS-CoV-2 S B.1.351 (Fig. 2B). Therefore, we concluded that the MCMV vector induces robust neutralization titers against multiple clinically-relevant SARS-CoV-2 variants. We next tested the dynamics of serum neutralization capacity against a bona fide SARS-CoV-2 isolate. Sera were incubated with SARS-CoV-2 and serum titers resulting in a 50% neutralization of virus (VNT_{50}) were determined. A part of each serum sample was pre-incubated with 2-mercaptoethanol (2-ME), which specifically destroys the neutralizing activity of IgM (57). Therefore, these samples essentially showed the neutralization capacity of the IgG antibody class, which is dominant in the serum. We observed that the neutralizing antibody titers against SARS-CoV-2 increased from an average VNT_{50} titer of 1:84 at 7 dpi to 1:476 at 56 dpi (Fig. 2C and Table 1) for the whole serum fraction and from values below the limit of detection at 7 dpi to 1:407 at 56 dpi for the IgG serum fraction. While 3 out of 29 sera (2 sera at 14 dpi and 1 at 56 dpi) did not show any neutralizing capacity (we assume that these mice were not properly immunized due to technical reasons), the vast majority of $MCMV^S$ treated mice showed a clear immunization effect (Fig. 2C and S2). On the other hand, $MCMV^{WT}$ and mock-immunized mice

showed no specific immune responses against SARS-CoV-2 at any time, suggesting that the protection was specifically induced by the expression of the S protein from the MCMV vector (Fig. S3).

Interestingly, neutralization titers in 2-ME treated groups were essentially comparable to those from untreated groups by dpi 28 (Fig. 2C and Table 1), arguing that the fraction of class-switched antibodies increased significantly at later time points. Furthermore, the antibody titer peaked at 28 dpi, while the neutralization capacity kept expanding until the last measured time point at 56 dpi. Taken together, these observations implied a robust germinal center reaction leading to somatic hypermutations and affinity maturation. We measured therefore the binding avidity of serum antibodies over time by sodium thiocyanate (NaSCN) inhibition (49, 58). Sera from MCMV^{S} immunized mice were treated by graded amounts of NaSCN and residual binding to S was determined by ELISA as indicator of avidity. Binding avidity increased consistently and continuously from 7 to 56 dpi (Fig. 2D and 2E). Therefore, the increase in neutralization capacity over time (Fig. 2C) was matched by an increase in binding avidity (Fig. 2D), rather than by an increase in the amount of antibodies (Fig. 2A).

Immunization with MCMV expressing the full-length HA protein induces neutralizing antibody responses.

To test if antibody responses can be elicited against another respiratory virus, we tested the hemagglutination inhibition (HAI) serum titers at 28 days post immunization with MCMV^{HA}. As control, we used the MCMV^{IVL}, an MCMV expressing solely an immunodominant MHC-I restricted octameric epitope from IAV HA (37). HA-specific antibodies were detected in MCMV^{HA} immunized mice, but not in those vaccinated with MCMV^{IVL} (Fig. 2F). Therefore, the MCMV vaccine vector expressing the full-length HA induced humoral responses that recognized HA and impaired its binding, and this was not due to cross reactivity to MCMV antigens, as seen in the MCMV^{IVL} control group.

MCMV^{HA} vaccination induces robust immune protection, but weak CD8$^+$ T cell responses

C57BL/6 mice were i.p. immunized with MCMV^{HA}. Control groups were not infected, or infected with the parental virus MCMV$^{\Delta m157}$ which lacks the *m157* gene, but does not express the HA gene. Mice were challenged with lethal IAV doses at 21 days post immunization and weight loss and mortality were followed. PBS immunized mice showed severe body weight loss and mortality, whereas MCMV^{HA} immunized mice showed no weight loss and no mortality (Fig. 3A and 3B). We compared the effects of immunization with Rae-1γMCMV^{HA} to the parental MCMV^{HA} and MCMV$^{\Delta m157}$ viruses by measuring weight loss kinetics for 5 days upon IAV challenge. We also measured flu virus titers in the lungs of challenged mice at 5 days post IAV challenge. While weight loss was averted in both groups immunized with MCMVs expressing the HA gene, and flu titers were reduced in the same groups relative to control mice that were immunized with MCMV$^{\Delta m157}$ or not immunized at all (Fig. S1B and S1C), Rae-1γMCMV^{HA} immunization did not reduce titers more efficiently than MCMV^{HA}. Hence, the MCMVs encoding HA provided immune protection against IAV challenge, irrespective of RAE1γ expression.

Since MCMV^{HA} provided immune protection even when applied i.p., whereas MCMV^{IVL} was protective only when applied i.n. (37), and since HAI titers were induced exclusively by MCMV^{HA} (Fig. 2F), we considered the possibility that MCMV^{HA} induces stronger adaptive immune responses than MCMV^{IVL}. Therefore, we compared IVL-specific K^d-restricted CD8$^+$ T-cell responses upon MCMV^{IVL} or MCMV^{HA} infection in BALB/c mice. We monitored the frequency of IFNγ$^+$ CD8$^+$ T cells until 115 dpi and observed that IFNγ$^+$ CD8$^+$ T-cell counts robustly increase in MCMV^{IVL} immunized mice, but barely in MCMV^{HA} immunized groups, both in relative and absolute terms (Fig. 3C). Similar responses were observed at 7 days post IAV challenge, where mice primed with MCMV^{IVL} showed substantially stronger cytokine responses in the CD8$^+$ compartment upon in vitro restimulation with the IVL peptide (Fig. 3D). Hence, our data indicated that superior protection provided by MCMV^{HA} may not be due to stronger cellular immunity.

To directly compare the protective capacity of MCMV^{IVL} and MCMV^{HA}, we challenged the mice with IAV at times of virus latency (>3 months post immunization) and measured the IAV titer in the lungs of immunized mice at 5 days post challenge. No infectious IAV could be detected in MCMV^{HA} immunized mice, whereas all MCMV^{IVL} immunized mice showed clearly detectable virus titers (Fig. 3E). We also monitored body weight upon IAV challenge and observed a significant drop in mice immunized with MCMV^{IVL} but not in those immunized with MCMV^{HA} (Fig. 3F). Intriguingly, only MCMV^{HA} immunized mice showed robust HAI serum titers at 5 days post IAV challenge (Fig. 3G). Therefore, our results suggested that the virus expressing the full-length HA gene provides better immune protection, likely due to humoral immune responses.

MCMV full-length-protein vector gives protection against viral challenge through humoral response.

While our results showed that MCMVs expressing viral glycoproteins induce neutralizing immunity, it was not formally proven that the humoral immunity was essential for immune protection upon challenge. To test this directly, we immunized B-cell deficient JHT mice with MCMV^{HA} and challenged them with IAV at 120 days post immunization (Fig. 4A). As expected, HA-specific antibodies were observed only in the immunized BALB/c mice, while no functional HA-specific antibodies could be detected in JHT mice (Fig. 4B). Similarly, viral titers were detected only in the lungs of vaccinated JHT mice, but were absent from BALB/c controls (Fig. 4C). Moreover, JHT mice suffered a significant weight loss upon IAV challenge whereas WT littermates did not (Fig. 4D). Taken together, these results indicated a critical role of antibodies in controlling IAV. Our data demonstrate that MCMVs expressing a full-length-protein provide immune protection against respiratory viral challenge and this protection depends on the humoral response of neutralizing antibodies.

Discussion

CMV has aroused great interest as a vaccine vector in recent years due to its strong immunogenicity and ability to establish life-long inflationary $CD8^+$ T cell-response (59). Many studies have demonstrated that exogenous antigens fused to the CMV genome provide protection against corresponding pathogens, but almost all of the previous publications handled T cell-based immune protection (17, 18, 20, 21, 28, 37) and barely covered B cell-based humoral responses, which prevent viral spread via extracellular fluids (60). One detailed study has shown that MCMVs induce protective humoral immune responses against a murine retrovirus (61), but it remained unclear if this principle applies to clinically relevant pathogens. Humoral immunity against the Ebola glycoprotein protein was observed upon immunization of rhesus monkeys with an RhCMV vector by ELISA, but the sera showed no virus neutralization capacity (21). In this study, we constructed MCMV-based vaccine vectors against two pandemic viruses, IAV and SARS-CoV-2, and demonstrated that neutralizing humoral immune responses against both are induced by recombinant MCMV vaccination, and that immune protection is abrogated in B-cell deficient mice. Humoral immunity elicited by $MCMV^{HA}$ provided better protection against IAV challenge than the robust cellular immunity elicited by $MCMV^{IVL}$. Furthermore, the insertion of Rae-1γ was previously shown to promote memory $CD8^+$ T-cell responses, thus improving protection by CMV vectors (39, 62, 63), but Rae-1γ did not improve $MCMV^{HA}$ protection against IAV challenge in this system, arguing against a role of T-cells in $MCMV^{HA}$ mediated protection. Taken together, our evidence strongly argues that humoral immunity was both sufficient and necessary to provide immune protection against respiratory virus challenge.

Previous results showed, however, that MCMV vectors expressing a single MHC-I restricted peptide are sufficient to provide protection against viral challenge (20, 28, 33, 35). Even more surprisingly, others and we have shown that MCMVs expressing a single immunodominant peptide provide better protection than those carrying the full-length protein (34, 64). Here we

observed the exactly opposite phenotype, where the full length protein provided better protection. However, systemic inflationary T-cell responses do not protect against influenza or respiratory syncytial virus (37, 44), and i.p. immunization, as performed in this study, does not elicit the protective lung mucosal $CD8^+$ T-cell responses. Therefore, our data may indicate that respiratory viral infections may be controlled better by systemic humoral immunity than by systemic cellular immunity.

Our study did not address the potential of CMV vectors to elicit mucosal humoral immunity and if it would provide better protection against IAV or SARS-CoV-2 infection. This question is intriguing, but goes beyond the scope of the present manuscript. Hence, it needs to be addressed in future studies, whether intranasal administration of MCMV vectors induces mucosal (IgA) antibody responses and if this would further improve immune protection.

Immediate early genes, especially ie1 and ie2 of MCMV, are sporadically expressed during the latency, enhancing the formation of memory inflation (65). A similar induction of humoral immunity against CMV antigens was documented in a previous study (49). We used ie promoters to express the S or HA proteins and observed an ongoing increase in the neutralizing capacity of sera up to 8 weeks post infection and robust immune protection at three months post immunization. One explanation for these phenomena may be the continuous restimulation of antigen-specific B cells by sparse antigen expression during latency, boosting B-cell immunity over time. While this hypothesis needs to be experimentally validated in future studies, our data demonstrate that the level of neutralizing antibodies increased over time, that the level of class-switched isotypes gradually increased and dominated at later time points after vaccination and that this was concomitant with an increase in avidity. All of these findings implicate somatic hypermutation processes upon germinal center reactions elicited by the MCMV vector immunization.

In summary, our data argue that a single injection of an MCMV vector may be sufficient to induce protective B-cell memory responses against respiratory viral pathogens, which is an improvement

over most among the currently available vaccine formulations against COVID-19. This also argues that CMV vectors might be used as vaccine tools against other pathogens that may emerge in the future. In light of observations that replication-deficient CMV vectors provide long-term immune protection (40, 42, 66), it is possible to envisage vaccine formulations that combine safety and long-term humoral immune protection. This study provides a crucial contribution in that direction.

Acknowledgments

We thank Inge Hollatz-Rangosch, Bettina Fürholzner, Martina Grashoff and Tatjana Hirsch for expert technical assistance and Susanne Talay and Andrea Kröger for advice and support. We thank Christine Goffinet for providing us the Vero-E6 cell line. This research was supported by the grant 14-76103-84 from the Ministry of Science and Culture of Lower Saxony to LCS, by the Helmholtz Association Eu Partnering grant MCMVaccine (PEI-008) to LCS and SJ, and by the European Union's Horizon 2020 research and innovation programme under grant agreement No 101003650 to MH.

Declaration of Interests

The authors declare no competing interest.

Reference

1. Chen JR, Ma C, Wong CH. Vaccine design of hemagglutinin glycoprotein against influenza. Trends Biotechnol. 2011;29(9):426-34.

2. Sriwilaijaroen N, Suzuki Y. Molecular basis of the structure and function of H1 hemagglutinin of influenza virus. Proc Jpn Acad Ser B Phys Biol Sci. 2012;88(6):226-49.

3. Cheng YW, Chao TL, Li CL, Chiu MF, Kao HC, Wang SH, et al. Furin Inhibitors Block SARS-CoV-2 Spike Protein Cleavage to Suppress Virus Production and Cytopathic Effects. Cell Rep. 2020:108254.

4. Hoffmann M, Kleine-Weber H, Pohlmann S. A Multibasic Cleavage Site in the Spike Protein of SARS-CoV-2 Is Essential for Infection of Human Lung Cells. Mol Cell. 2020;78(4):779-84 e5.

5. Zhao P, Praissman JL, Grant OC, Cai Y, Xiao T, Rosenbalm KE, et al. Virus-Receptor Interactions of Glycosylated SARS-CoV-2 Spike and Human ACE2 Receptor. Cell Host Microbe. 2020;28(4):586-601 e6.

6. Hoffmann M, Kleine-Weber H, Schroeder S, Kruger N, Herrler T, Erichsen S, et al. SARS-CoV-2 Cell Entry Depends on ACE2 and TMPRSS2 and Is Blocked by a Clinically Proven Protease Inhibitor. Cell. 2020;181(2):271-80 e8.

7. WHO. Draft landscape of COVID-19 candidate vaccines. World Health Organization2020.

8. Krammer F. SARS-CoV-2 vaccines in development. Nature. 2020.

9. Sahin U, Muik A, Derhovanessian E, Vogler I, Kranz LM, Vormehr M, et al. COVID-19 vaccine BNT162b1 elicits human antibody and T(H)1 T cell responses. Nature. 2020;586(7830):594-9.

10. Mahase E. Covid-19: UK approves Pfizer and BioNTech vaccine with rollout due to start next week. Bmj. 2020;371:m4714.

11. WHO. WHO regional office for Europe. Seasonal influenza2021.

12. CDC. CDC seasonal Flu Vaccine Effectiveness studies. Centers for Disease Control and Prevention2021.

13. Dawood FS, Chung JR, Kim SS, Zimmerman RK, Nowalk MP, Jackson ML, et al. Interim Estimates of 2019-20 Seasonal Influenza Vaccine Effectiveness - United States, February 2020. MMWR Morb Mortal Wkly Rep. 2020;69(7):177-82.

14. Coffman RL, Sher A, Seder RA. Vaccine adjuvants: putting innate immunity to work. Immunity. 2010;33(4):492-503.

15. Ura T, Okuda K, Shimada M. Developments in Viral Vector-Based Vaccines. Vaccines (Basel). 2014;2(3):624-41.

16. Lauer KB, Borrow R, Blanchard TJ. Multivalent and Multipathogen Viral Vector Vaccines. Clinical and vaccine immunology : CVI. 2017;24(1).

17. Lillie PJ, Berthoud TK, Powell TJ, Lambe T, Mullarkey C, Spencer AJ, et al. Preliminary assessment of the efficacy of a T-cell-based influenza vaccine, MVA-NP+M1, in humans. Clinical infectious diseases : an official publication of the Infectious Diseases Society of America. 2012;55(1):19-25.

18. Hansen SG, Ford JC, Lewis MS, Ventura AB, Hughes CM, Coyne-Johnson L, et al. Profound early control of highly pathogenic SIV by an effector memory T-cell vaccine. Nature. 2011;473(7348):523-7.

19. Price GE, Soboleski MR, Lo CY, Misplon JA, Quirion MR, Houser KV, et al. Single-dose mucosal immunization with a candidate universal influenza vaccine provides rapid protection from virulent H5N1, H3N2 and H1N1 viruses. PloS one. 2010;5(10):e13162.

20. Hansen SG, Vieville C, Whizin N, Coyne-Johnson L, Siess DC, Drummond DD, et al. Effector memory T cell responses are associated with protection of rhesus monkeys from mucosal simian immunodeficiency virus challenge. Nat Med. 2009;15(3):293-9.

21. Marzi A, Murphy AA, Feldmann F, Parkins CJ, Haddock E, Hanley PW, et al. Cytomegalovirus-based vaccine expressing Ebola virus glycoprotein protects nonhuman primates from Ebola virus infection. Scientific reports. 2016;6:21674.

22. Alharbi NK, Padron-Regalado E, Thompson CP, Kupke A, Wells D, Sloan MA, et al. ChAdOx1 and MVA based vaccine candidates against MERS-CoV elicit neutralising antibodies and cellular immune responses in mice. Vaccine. 2017;35(30):3780-8.

23. Koch T, Dahlke C, Fathi A, Kupke A, Krahling V, Okba NMA, et al. Safety and immunogenicity of a modified vaccinia virus Ankara vector vaccine candidate for Middle East respiratory syndrome: an open-label, phase 1 trial. Lancet Infect Dis. 2020;20(7):827-38.

538 24. Volz A, Kupke A, Song F, Jany S, Fux R, Shams-Eldin H, et al. Protective Efficacy of Recombinant
539 Modified Vaccinia Virus Ankara Delivering Middle East Respiratory Syndrome Coronavirus Spike
540 Glycoprotein. J Virol. 2015;89(16):8651-6.
541 25. Kim MH, Kim HJ, Chang J. Superior immune responses induced by intranasal immunization with
542 recombinant adenovirus-based vaccine expressing full-length Spike protein of Middle East respiratory
543 syndrome coronavirus. PloS one. 2019;14(7):e0220196.
544 26. Karrer U, Sierro S, Wagner M, Oxenius A, Hengel H, Koszinowski UH, et al. Memory inflation:
545 continuous accumulation of antiviral CD8+ T cells over time. Journal of immunology. 2003;170(4):2022-9.
546 27. Munks MW, Cho KS, Pinto AK, Sierro S, Klenerman P, Hill AB. Four Distinct Patterns of Memory
547 CD8 T Cell Responses to Chronic Murine Cytomegalovirus Infection. The Journal of Immunology.
548 2006;177(1):450-8.
549 28. Karrer U, Wagner M, Sierro S, Oxenius A, Hengel H, Dumrese T, et al. Expansion of protective CD8+
550 T-cell responses driven by recombinant cytomegaloviruses. J Virol. 2004;78(5):2255-64.
551 29. Holtappels R, Pahl-Seibert MF, Thomas D, Reddehase MJ. Enrichment of immediate-early 1
552 (m123/pp89) peptide-specific CD8 T cells in a pulmonary CD62L(lo) memory-effector cell pool during
553 latent murine cytomegalovirus infection of the lungs. J Virol. 2000;74(24):11495-503.
554 30. Holtappels R, Thomas D, Podlech J, Reddehase MJ. Two antigenic peptides from genes m123 and
555 m164 of murine cytomegalovirus quantitatively dominate CD8 T-cell memory in the H-2d haplotype. J
556 Virol. 2002;76(1):151-64.
557 31. Sylwester AW, Mitchell BL, Edgar JB, Taormina C, Pelte C, Ruchti F, et al. Broadly targeted human
558 cytomegalovirus-specific CD4+ and CD8+ T cells dominate the memory compartments of exposed
559 subjects. J Exp Med. 2005;202(5):673-85.

32. Cicin-Sain L, Sylwester AW, Hagen SI, Siess DC, Currier N, Legasse AW, et al. Cytomegalovirus-specific T cell immunity is maintained in immunosenescent rhesus macaques. Journal of immunology. 2011;187(4):1722-32.

33. Borkner L, Sitnik KM, Dekhtiarenko I, Pulm AK, Tao R, Drexler I, et al. Immune Protection by a Cytomegalovirus Vaccine Vector Expressing a Single Low-Avidity Epitope. Journal of immunology. 2017;199(5):1737-47.

34. Dekhtiarenko I, Ratts RB, Blatnik R, Lee LN, Fischer S, Borkner L, et al. Peptide Processing Is Critical for T-Cell Memory Inflation and May Be Optimized to Improve Immune Protection by CMV-Based Vaccine Vectors. PLoS pathogens. 2016;12(12):e1006072.

35. Tsuda Y, Caposio P, Parkins CJ, Botto S, Messaoudi I, Cicin-Sain L, et al. A replicating cytomegalovirus-based vaccine encoding a single Ebola virus nucleoprotein CTL epitope confers protection against Ebola virus. PLoS neglected tropical diseases. 2011;5(8):e1275.

36. Tsuda Y, Parkins CJ, Caposio P, Feldmann F, Botto S, Ball S, et al. A cytomegalovirus-based vaccine provides long-lasting protection against lethal Ebola virus challenge after a single dose. Vaccine. 2015;33(19):2261-6.

37. Zheng X, Oduro JD, Boehme JD, Borkner L, Ebensen T, Heise U, et al. Mucosal CD8+ T cell responses induced by an MCMV based vaccine vector confer protection against influenza challenge. PLoS pathogens. 2019;15(9):e1008036.

38. Hirsl L, Brizic I, Jenus T, Juranic Lisnic V, Reichel JJ, Jurkovic S, et al. Murine CMV Expressing the High Affinity NKG2D Ligand MULT-1: A Model for the Development of Cytomegalovirus-Based Vaccines. Front Immunol. 2018;9:991.

39. Slavuljica I, Busche A, Babic M, Mitrovic M, Gasparovic I, Cekinovic D, et al. Recombinant mouse cytomegalovirus expressing a ligand for the NKG2D receptor is attenuated and has improved vaccine properties. The Journal of clinical investigation. 2010;120(12):4532-45.

584 40. Snyder CM, Allan JE, Bonnett EL, Doom CM, Hill AB. Cross-presentation of a spread-defective
585 MCMV is sufficient to prime the majority of virus-specific CD8+ T cells. PloS one. 2010;5(3):e9681.
586 41. Cicin-Sain L, Bubic I, Schnee M, Ruzsics Z, Mohr C, Jonjic S, et al. Targeted deletion of regions rich
587 in immune-evasive genes from the cytomegalovirus genome as a novel vaccine strategy. J Virol.
588 2007;81(24):13825-34.
589 42. Mohr CA, Arapovic J, Mühlbach H, Panzer M, Weyn A, Dölken L, et al. A spread-deficient
590 cytomegalovirus for assessment of first-target cells in vaccination. J Virol. 2010;84(15):7730-42.
591 43. Tamura M, Kuwano K, Kurane I, Ennis FA. Definition of amino acid residues on the epitope
592 responsible for recognition by influenza A virus H1-specific, H2-specific, and H1- and H2-cross-reactive
593 murine cytotoxic T-lymphocyte clones. J Virol. 1998;72(11):9404-6.
594 44. Morabito KM, Ruckwardt TR, Redwood AJ, Moin SM, Price DA, Graham BS. Intranasal
595 administration of RSV antigen-expressing MCMV elicits robust tissue-resident effector and effector
596 memory CD8+ T cells in the lung. Mucosal immunology. 2017;10(2):545-54.
597 45. Chaudhry MZ, Messerle M, Cicin-Sain L. Construction of Human Cytomegalovirus Mutants with
598 Markerless BAC Mutagenesis. Methods in molecular biology. 2021;2244:133-58.
599 46. Dag F, Dolken L, Holzki J, Drabig A, Weingartner A, Schwerk J, et al. Reversible silencing of
600 cytomegalovirus genomes by type I interferon governs virus latency. PLoS pathogens.
601 2014;10(2):e1003962.
602 47. Chaudhry MZ, Eschke K, Grashoff M, Abassi L, Kim Y, Brunotte L, et al. SARS-CoV-2 Quasispecies
603 Mediate Rapid Virus Evolution and Adaptation. bioRxiv. 2020:2020.08.10.241414.
604 48. Bertoglio F, Meier D, Langreder N, Steinke S, Rand U, Simonelli L, et al. SARS-CoV-2 neutralizing
605 human recombinant antibodies selected from pre-pandemic healthy donors binding at RBD-ACE2
606 interface. 2020:2020.06.05.135921.

607 49. Welten SPM, Redeker A, Toes REM, Arens R. Viral Persistence Induces Antibody Inflation without
608 Altering Antibody Avidity. J Virol. 2016;90(9):4402-11.
609 50. Madhun AS, Akselsen PE, Sjursen H, Pedersen G, Svindland S, Nostbakken JK, et al. An adjuvanted
610 pandemic influenza H1N1 vaccine provides early and long term protection in health care workers. Vaccine.
611 2010;29(2):266-73.
612 51. Kleine-Weber H, Elzayat MT, Wang L, Graham BS, Müller MA, Drosten C, et al. Mutations in the
613 Spike Protein of Middle East Respiratory Syndrome Coronavirus Transmitted in Korea Increase Resistance
614 to Antibody-Mediated Neutralization. J Virol. 2019;93(2).
615 52. Hoffmann M, Arora P, Groß R, Seidel A, Hörnich B, Hahn A, et al. SARS-CoV-2 variants B.1.351 and
616 B.1.1.248: Escape from therapeutic antibodies and antibodies induced by infection and vaccination.
617 2021:2021.02.11.430787.
618 53. Berger Rentsch M, Zimmer G. A vesicular stomatitis virus replicon-based bioassay for the rapid
619 and sensitive determination of multi-species type I interferon. PloS one. 2011;6(10):e25858.
620 54. Blazejewska P, Koscinski L, Viegas N, Anhlan D, Ludwig S, Schughart K. Pathogenicity of different
621 PR8 influenza A virus variants in mice is determined by both viral and host factors. Virology.
622 2011;412(1):36-45.
623 55. Bubić I, Wagner M, Krmpotić A, Saulig T, Kim S, Yokoyama WM, et al. Gain of virulence caused by
624 loss of a gene in murine cytomegalovirus. J Virol. 2004;78(14):7536-44.
625 56. Cardin RD, Abenes GB, Stoddart CA, Mocarski ES. Murine cytomegalovirus IE2, an activator of
626 gene expression, is dispensable for growth and latency in mice. Virology. 1995;209(1):236-41.
627 57. Capel PJ, Gerlag PG, Hagemann JF, Koene RA. The effect of 2-mercaptoethanol on IgM and IgG
628 antibody activity. J Immunol Methods. 1980;36(1):77-80.

58. Suwannalai P, Scherer HU, van der Woude D, Ioan-Facsinay A, Jol-van der Zijde CM, van Tol MJ, et al. Anti-citrullinated protein antibodies have a low avidity compared with antibodies against recall antigens. Ann Rheum Dis. 2011;70(2):373-9.

59. Ynga-Durand MA, Dekhtiarenko I, Cicin-Sain L. Vaccine Vectors Harnessing the Power of Cytomegaloviruses. Vaccines (Basel). 2019;7(4).

60. Murphy K, Travers P, Walport M, Janeway C. Janeway's immunobiology. New York: Garland Science; 2008.

61. Bongard N, Le-Trilling VTK, Malyshkina A, Rückborn M, Wohlgemuth K, Wensing I, et al. Immunization with a murine cytomegalovirus based vector encoding retrovirus envelope confers strong protection from Friend retrovirus challenge infection. PLoS pathogens. 2019;15(9):e1008043.

62. Trsan T, Busche A, Abram M, Wensveen FM, Lemmermann NA, Arapovic M, et al. Superior induction and maintenance of protective CD8 T cells in mice infected with mouse cytomegalovirus vector expressing RAE-1gamma. Proc Natl Acad Sci U S A. 2013;110(41):16550-5.

63. Slavuljica I, Krmpotic A, Jonjic S. Manipulation of NKG2D ligands by cytomegaloviruses: impact on innate and adaptive immune response. Front Immunol. 2011;2:85.

64. Klyushnenkova EN, Kouiavskaia DV, Parkins CJ, Caposio P, Botto S, Alexander RB, et al. A cytomegalovirus-based vaccine expressing a single tumor-specific CD8+ T-cell epitope delays tumor growth in a murine model of prostate cancer. Journal of immunotherapy (Hagerstown, Md : 1997). 2012;35(5):390-9.

65. Seckert CK, Griessl M, Buttner JK, Scheller S, Simon CO, Kropp KA, et al. Viral latency drives 'memory inflation': a unifying hypothesis linking two hallmarks of cytomegalovirus infection. Medical microbiology and immunology. 2012;201(4):551-66.

66. Hansen SG, Marshall EE, Malouli D, Ventura AB, Hughes CM, Ainslie E, et al. A live-attenuated RhCMV/SIV vaccine shows long-term efficacy against heterologous SIV challenge. Sci Transl Med. 2019;11(501).

Figure Legends

Figure 1. Generation of recombinant MCMV vectors.

(A-B) Schematic images of the recombinant MCMV vector genome. (A) The HA gene of IAV PR8 was inserted along with minimal hMIEP in the m157 locus. (B) The SARS-CoV-2 spike ORF was inserted in place of ie2. (C-D) Western blots of purified virus stocks of $MCMV^{S}$, $MCMV^{HA}$ and $MCMV^{WT}$ were performed with antibodies against (C) IAV HA or (D) the SARS CoV-2 S. As controls we used (C) IE1 or (D) MCK-2 proteins of MCMV.

Figure 2. Immunization with $MCMV^{S}$ and $MCMV^{HA}$ elicits antigen-specific and neutralizing humoral responses

(A-E) BALB/c mice were infected with $2x10^5$ PFU of $MCMV^{S}$ via the i.p. route. Collected sera were tested for antigen-specific responses and neutralization capacity. (A) EC_{50} of IgG isotypes specific for S1-S2 or RBD. Each symbol indicates an individual mouse, means from individual time points are connected with lines. (B) Pseudovirus neutralization capacity (pVNT) against the SARS-CoV-2 S WH01+D614G, B.1.1.7 and B.1.351 variants. The assay was performed in technical triplicates and mean values for each mouse serum are shown, where each symbol represents the percentage of neutralization of a mouse serum sample at 56 dpi. Values were calculated by luciferase units. Lines connect the group averages for each serum dilution step. (C) Neutralization capacity against SARS-CoV-2 (VNT_{50}) of total serum immunoglobulins (total Ig) or their IgG fraction (IgG only) at indicated time points post immunization. Each symbol indicates sera from one mouse and lines connect means for each time point. (D) Percentage of serum antibodies

binding to the S protein (y axis), in the presence of increasing concentrations of NaSCN (x axis) and normalized to ELISA values in absence of NaSCN. Each line connects the average residual binding at indicated molar concentrations of NaSCN. Error bars are standard deviations (SD). (E) Percentage of residual antibodies binding to S in the presence of 1M NaSCN. The assay was performed in biological triplicates as in panel D and data from indicated time points post immunization were statistically compared by one-way ANOVA. *** $p<0.001$ (F) Titers of HA-specific antibodies at 28 dpi with $MCMV^{HA}$ or $MCMV^{IVL}$. Data were pooled from two independent experiments. Long horizontal lines indicate means. Mann-Whitney U test was used for statistical analysis *** $p<0.001$.

Figure 3. $MCMV^{HA}$ immunization induces robust immune protection, but poor IVL-specific $CD8^+$ T-cell response

(A-B) C57BL/6 female mice were immunized with $2x10^5$ PFU of $MCMV^{HA}$ or $MCMV^{\Delta m157}$ virus via the f.p. route. After 21 days, mice were challenged with IAV (100 HU). (A) Body weight loss and (B) survival rates were measured. (C-G) BALB/c mice were infected with $2x10^5$ PFU of $MCMV^{HA}$ or $MCMV^{IVL}$ via the i.p. route. (C) Blood leukocytes were isolated and stimulated *in vitro* with IVL-peptide for 6h and analyzed by intracellular cytokine staining (ICCS) in flow cytometry at indicated dpi. Percentages and cell counts of IVL-specific $CD8^+$ T cells in peripheral blood are shown as averages +/- SD (n=6-10) (D-G) Immunized mice were challenged with IAV (1100 FFU, i.n.) at > 3 months p.i. Blood leukocytes were *in vitro* stimulated with the IVL-peptide for 6h and analyzed by ICCS in flow cytometry on day 8 post challenge. Each symbol represents an individual mouse sample. (E) IAV titers measure by focus-forming assay (FFA) in the lungs on day 5 post challenge. Each symbol represents an individual mouse. (F) Average body weight loss upon IAV challenge at indicated time points (n=6-9). (G) Titers of HA-specific antibodies in serum samples on day 5 after IAV challenge. Titers were detected by HA inhibition assay, n=6-9. Each symbol represents

an individual mouse. All of above data are pooled data from two independent experiments. Mann-Whitney U test were used for statistical analysis ** p<0.01, *** p<0.001, **** p<0.0001.

Figure 4. Humoral immunity elicited by MCMV^{HA} protects against IAV challenge.

JHT and BALB/c mice were immunized with 2x10^5 PFU of MCMV^{HA} via the i.p. route. 120 days after immunization, mice were challenged with IAV (1100 FFU, i.n.). (A) Setup of the experiment. (B) Titers of HA-specific antibody in serum samples on day 5 after IAV challenge determined by HAI. (C) IAV lung titers on day 5 post challenge. (D) Body weight loss upon IAV challenge. All data are pooled data from two independent experiments. Each symbol represents an individual mouse sample. Horizontal lines indicate means and error bars indicate standard error. Two-Way ANOVA for Fig. 5D or Mann-Whitney U test for Fig. 5B and 5C were used for statistical analysis. ** p<0.01, *** p<0.001, **** p<0.0001.

Table Legends

Table 1. VNT_{50} of MCMV^S immunized mouse serum samples against SARS-CoV-2 or pseudotyped VSV-S.

The table indicates average VNT_{50} or $pVNT_{50}$ values against SARS-CoV-2 or pseudotyped VSV-S of serum samples collected from immunized mice at indicated time points. Neutralizing antibody titers were calculated by nonlinear IC50 regression analysis in GraphPad Prism 9. The indicated VNT_{50} or $pVNT_{50}$ values denote the serum dilution that results in a 50% reduction of virus plaques or of VSV luciferase activity.

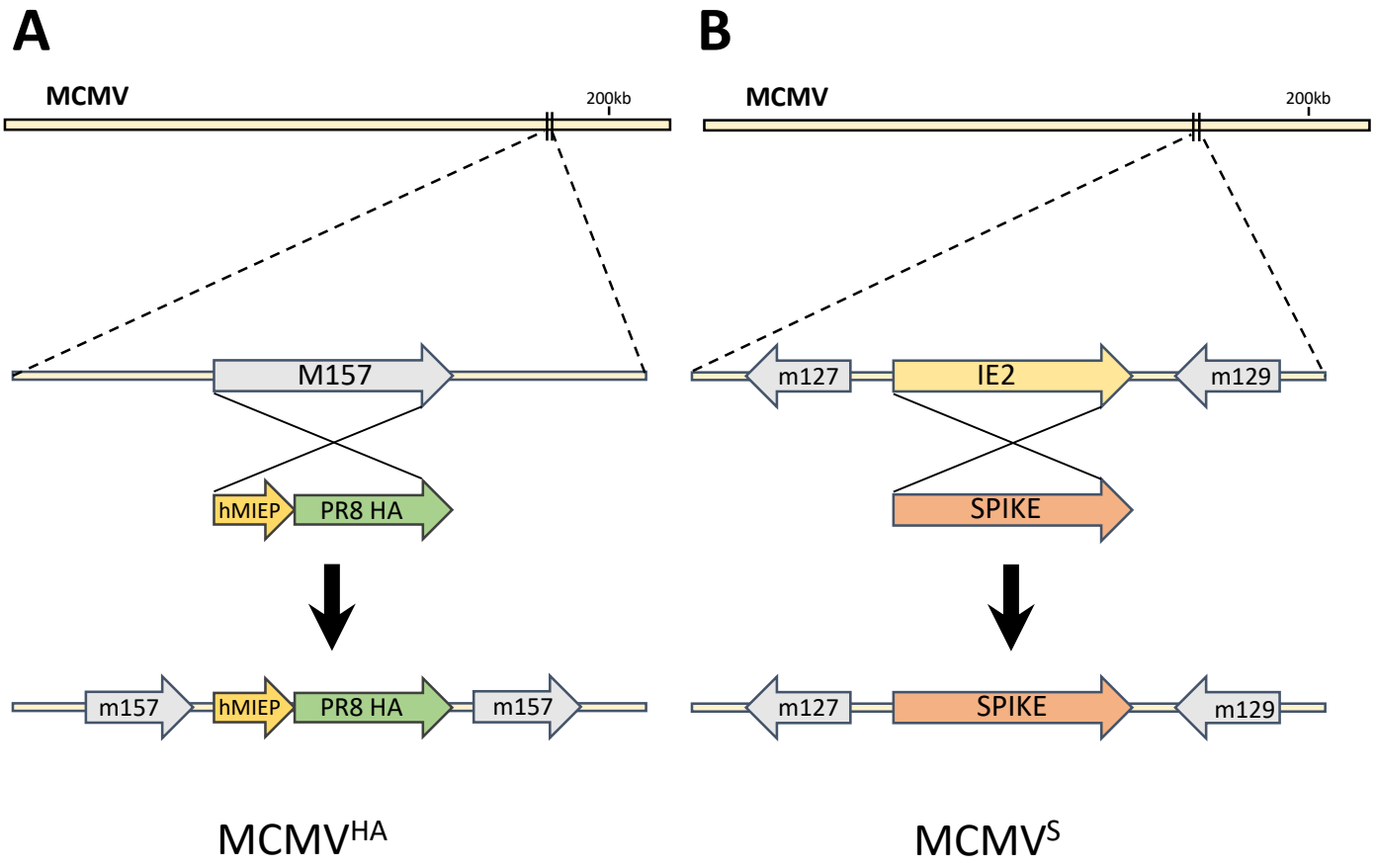
A
MCMV
200kb
M157
hMIEP
PR8 HA
m157
hMIEP
PR8 HA
m157
MCMV^HA
B
MCMV
200kb
m127
IE2
m129
SPIKE
m127
SPIKE
m129
MCMV^S

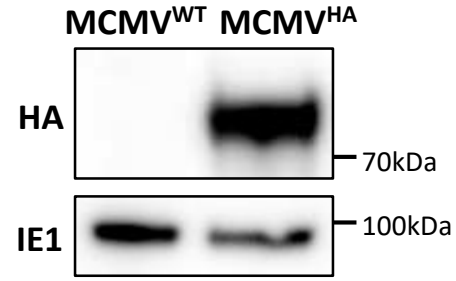
C
MCMV^WT MCMV^HA
HA
70kDa
IE1
100kDa

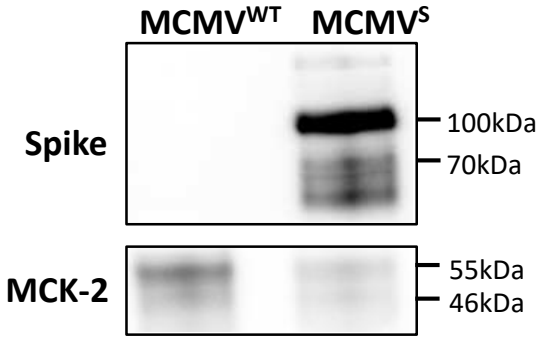
D
MCMV^WT MCMV^S
Spike
100kDa
70kDa
MCK-2
55kDa
46kDa

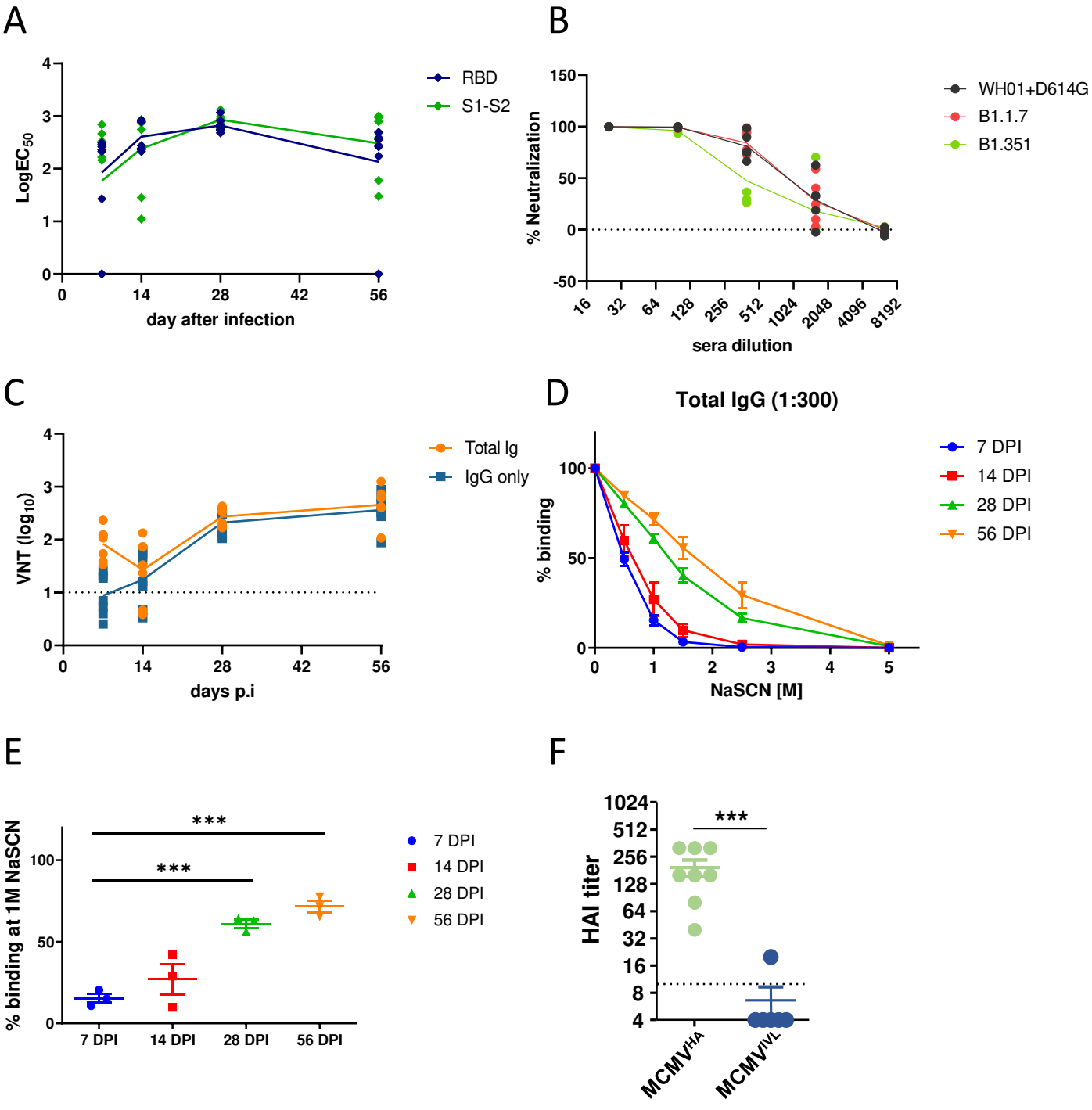
A
LogEC50
day after infection
RBD
S1-S2
B
% Neutralization
sera dilution
WH01+D614G
B1.1.7
B1.351
C
VNT (log10)
days p.i
Total Ig
IgG only
D
Total IgG (1:300)
% binding
NaSCN [M]
7 DPI
14 DPI
28 DPI
56 DPI
E
% binding at 1M NaSCN
***
***
7 DPI
14 DPI
28 DPI
56 DPI
F
HAI titer
***
MCMVIHA
MCMVIVL

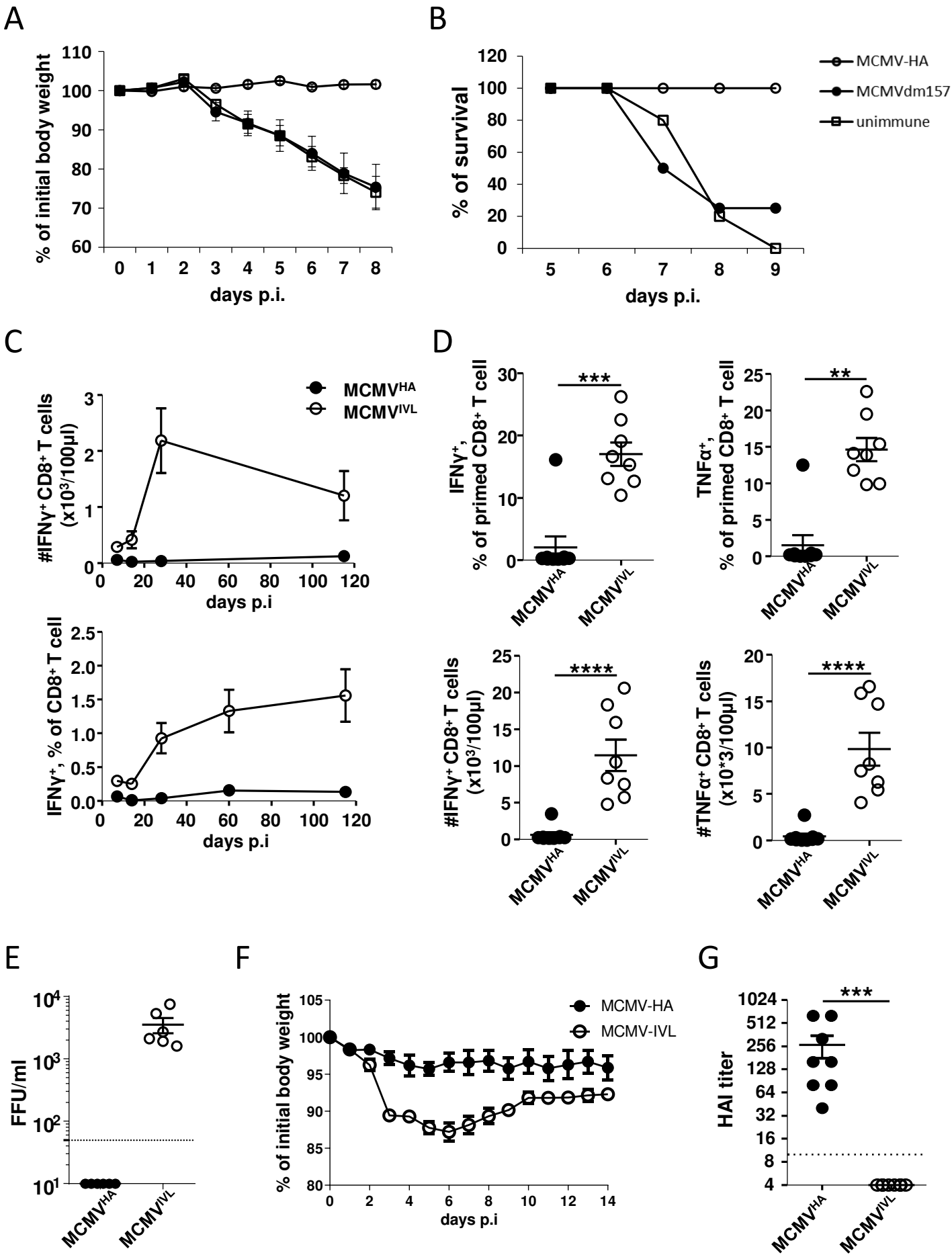
A
% of initial body weight
days p.i.
B
% of survival
days p.i.
MCMV-HA
MCMVdm157
unimmune
C
#IFNγ+ CD8+ T cells (x10³/100µl)
MCMV^HA
MCMV^IVL
days p.i
IFNγ+, % of CD8+ T cell
days p.i
D
IFNγ+, % of primed CD8+ T cell
TNFα+, % of primed CD8+ T cell
#IFNγ+ CD8+ T cells (x10³/100µl)
#TNFα+ CD8+ T cells (x10*3/100µl)
E
FFU/ml
F
% of initial body weight
days p.i
MCMV-HA
MCMV-IVL
G
HAI titer

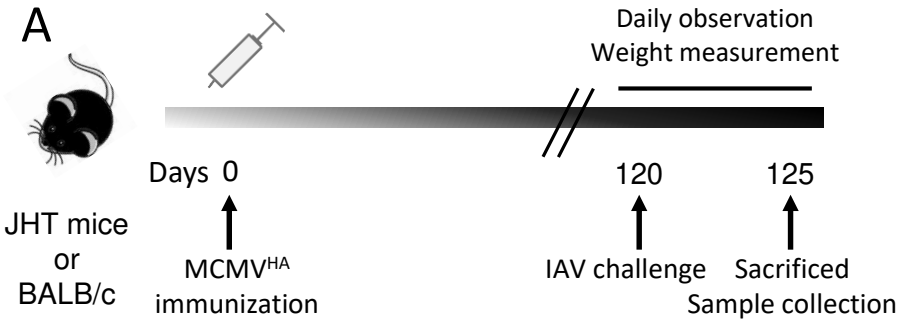
A
Daily observation
Weight measurement
Days 0
120
125
JHT mice
or
BALB/c
MCMV^HA
immunization
IAV challenge
Sacrificed
Sample collection

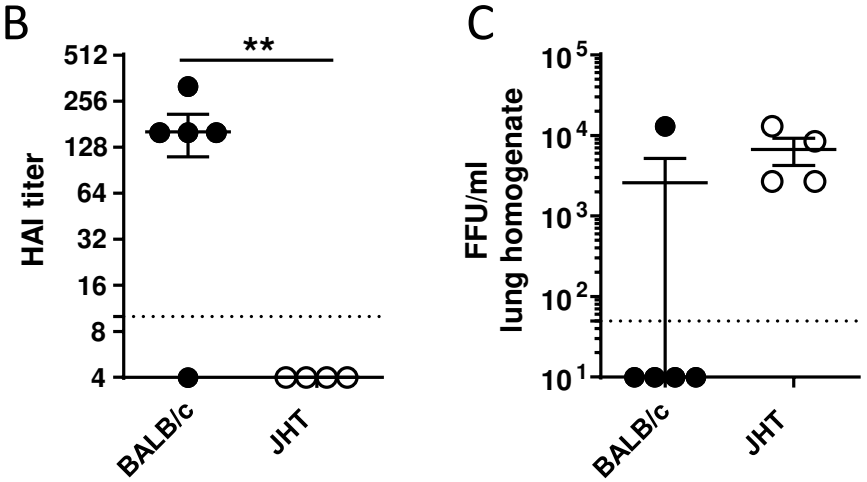
B
**
HAI titer
512
256
128
64
32
16
8
4
BALB/c
JHT
C
FFU/ml
lung homogenate
10^5
10^4
10^3
10^2
10^1
BALB/c
JHT

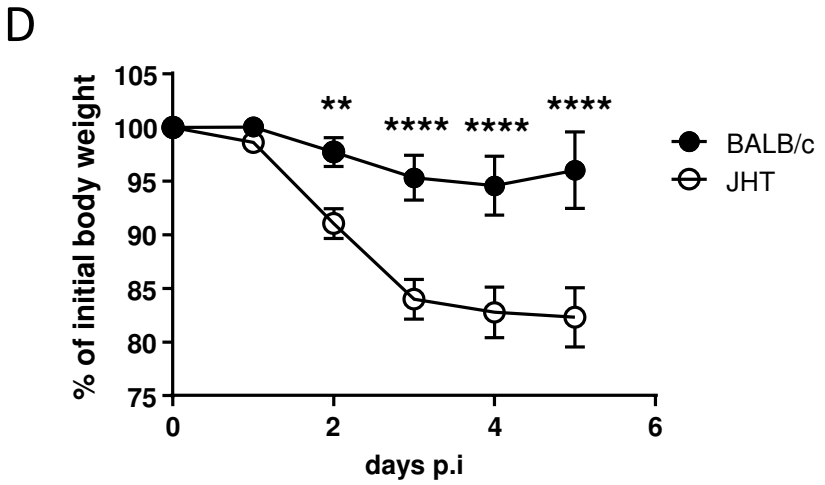
D
% of initial body weight
105
100
95
90
85
80
75
**
****
****
****
0
2
4
6
days p.i
BALB/c
JHT

Supplementary Files

This is a list of supplementary files associated with this preprint. Click to download.

- Table1.xlsx
- SupplementaryFigure.pdf
- Supplementaryfigurelegends.pdf